Available online at www.sciencedirect.com
ScienceDirect
Earth and Planetary Science Letters 262 (2007) 273–283
EPSL
www.elsevier.com/locate/epsl

Diamond-bearing COHS fluids in the mantle beneath Hawaii

Maria-Luce Frezzotti [a,*], Angelo Peccerillo [b]

[a] Dipartimento di Scienze della Terra, Università di Siena, Via Laterina 8, 53100, Siena, Italy
[b] Dipartimento di Scienze della Terra, Università di Perugia, P.za Università 1, 06100, Perugia, Italy

Received 22 November 2006; received in revised form 2 August 2007; accepted 6 August 2007
Available online 14 August 2007
Editor: R.W. Carlson

Abstract

We apply Raman microspectroscopy to exceptionally high-density CO_2 ($+H_2O+H_2S$) fluid inclusions containing nanocrystalline diamonds, which are present in garnet pyroxenites from Salt Lake Crater from Oahu (Hawaii), and show for the first time the presence of free diamond-bearing carbonate-rich fluids/melts, originated within the asthenospheric mantle at depths greater than 150 km, in the diamond stability field. We argue that these fluids can migrate, generate compositional and rheological modifications to form small-scale fluid-rich regions beneath Hawaii, which are easily melted to give enriched basaltic magmas at normal mantle temperatures.

Keywords: CO_2; carbonate-rich melt; water; diamond; fluid inclusions; pyroxenite; Hawaii

1. Introduction

Earth's mantle fluids are important for element transport between the mantle, the crust and finally the atmosphere. They influence the stability of many mantle phases, exert a strong influence on mantle rheology, and control melting of peridotites. C, O, H, S, and halogens represent the dominant volatiles in the Earth's mantle, either as fluid phases, or dissolved within silicate-melts, or as carbonate-rich liquids.

In the shallow mantle, there is ample natural and experimental evidence that CO_2-rich fluids dominate (Roedder, 1984; Gudfinnsson and Presnall, 2005), and that small quantities of H_2O occur stored in hydrous phases and/or dissolved in nominally anhydrous minerals (Thompson, 1992; Aubaud et al., 2004). CO_2-rich fluid inclusions are tremendously abundant in shallow mantle rocks worldwide (for a review, see Andersen and Neumann, 2001), which might in some cases be associated to carbonate-melt inclusions (Frezzotti et al., 2002a; Kamenetsky et al., 2004). Water-rich fluid inclusions have not been reported in xenoliths, with a few interesting exceptions related to subduction-zone settings (Roedder, 1965; Schiano et al., 1995).

At depths >120–150 km, the direct observation of fluids is rare, and come from sub-micrometer inclusions in cratonic diamonds, which might contain fluid and/or melt, or something intermediate (i.e. above the second critical end point in the relevant system, e.g. Wyllie and Ryabchikov, 2000), showing a continuous compositional

* Corresponding author. Tel.: +39 0577 233929; fax: +39 0577 233938.
E-mail addresses: frezzottiml@unisi.it (M.-L. Frezzotti), pecceang@unipg.it (A. Peccerillo).

0012-821X/$ - see front matter © 2007 Elsevier B.V. All rights reserved.
doi:10.1016/j.epsl.2007.08.001

variation between a carbonate and a hydrous silicate-rich end member (Navon et al., 1988; Izraeli et al., 2004; Klein-Ben David et al., 2006).

In intraplate oceanic settings, a precise characterization of the nature and role of mantle fluids may represent a way to explain the geochemical features of oceanic island basalts and the physicochemical characteristics of their mantle sources (Sen et al., 1996; Dixon and Clague, 2001). Fluid inclusions contained in mantle peridotites represent the main source of direct information about mantle fluid composition. Here, we report observation of CO_2–H_2O–H_2S fluid inclusions containing nanocrystalline diamonds in garnet pyroxenite samples from Oahu, Hawaii. Nano-diamonds have been previously reported in similar garnet pyroxenites, and interpreted as crystallized from metasomatic "basaltic" melts rich in volatiles (Wirth and Rocholl, 2003).

Present discovery of diamond bearing COHS fluids testifies for the presence of water-bearing carbonate-rich melts generated in the asthenosphere at depths greater than 150 km. Such fluids could play a major role for the formation of fertile lithospheric mantle sources at normal mantle temperatures, and could profoundly impact the mechanical characteristics of the lithosphere–asthenosphere system in oceanic intraplate settings.

2. Sample description

Post-erosional alkalic lavas of the Honolulu Volcanics (HV) series erupted from Salt Lake Crater crop out on the apron of the Koolau shield volcano on Oahu (Hawaii), and contain a rather unique series of rocks representing the oceanic mantle. They include spinel lherzolites, and spinel and garnet pyroxenites derived from the lithosphere beneath Hawaii, at depths greater that 60 km (Sen, 1988).

Studied garnet pyroxenite xenoliths consist of eight samples from the Dale Jackson Collection, on loan from the National Museum of Natural History (Smithsonian Institutions). Rocks consist mostly of clinopyroxene (diopside–augite, 60–70 vol.%), with subordinate orthopyroxene, olivine and garnet. They show coarse equigranular textures, and are anhydrous, although rare amphibole (pargasite) and/or phlogopite has been reported in similar pyroxenites (Sen et al., 1996). Garnet is of secondary origin, and mainly formed through exsolution from pyroxene during recrystallization processes. A more detailed xenolith's petrography is reported in Frezzotti et al. (1992). The genetic history of such rocks may be summarized as deep magmatic cumulates within the Hawaiian mantle from alkali–basaltic magmas isotopically similar to the HV series. (Sen, 1988) indicated equilibration conditions at 1000–1150 °C and 1.6–2.5 GPa. New studies (Sen et al., 2005; Keshav et al., in press) argue that garnet pyroxenites represent high-pressure cumulates at pressures above 3 GPa, and probably up to 5 GPa, based on *liquidus* phase relations in CMAS system ($P \geq 3$ GPa).

Within the clinopyroxene and orthopyroxene crystals, early fluid inclusions with regular shape (3–50 μm) occur isolated (Fig. 1a, b), or form short trails (Fig. 1c) outlining crystallographic directions. In clinopyroxene, many early inclusions are cut by spinel exsolution, as reported in Fig. 1a; such features represent unambiguous textural evidence for inclusion formation prior to cooling and re-equilibration of host rocks. Early fluid inclusions are generally CO_2-rich, similar to most inclusions in mantle xenoliths from oceanic mantle. They are commonly encircled by micro-fractures, characteristic of decrepitation (i.e. explosion due to fluid overpressure; Fig. 1a and b), but a few of the tiniest inclusions (<6–8 μm) still preserve a pristine high-density fluid phase.

Previous Raman and microthermometric studies indicated that inclusions contain high-density to super-dense CO_2, with densities up to 1.21 g/cm^3– the highest ever recorded by fluid inclusions in mantle peridotites– corresponding to a minimum pressure of 1.8–2 GPa, at the inferred mantle temperatures (Frezzotti et al., 1992).

Rare tiny (<5–6 μm) carbonate inclusions, and mixed CO_2 + carbonate ± diamond inclusions have been observed in association with early high-density CO_2 inclusions (Fig. 1d). Carbonate inclusions are high-birefringent single minerals, and show rounded shapes (i.e. droplets), as if they originally trapped a carbonate-rich melt phase (Fig. 1d). Carbonate inclusions do not show decrepitation features. Occasionally, decrepitation is observed limited to inclusions containing carbonate + CO_2.

All mineral phases further contain numerous late CO_2 fluid inclusions along intergranular microfractures; these were not considered in the present study since they represent late fluid processes, related to the ascent of xenoliths within host alkali–basalts.

3. Raman microspectroscopy study

Laser-Raman spectroscopy in single fluid inclusions was performed with a Labram microspectrometer of the Horiba Jobin Yvon, ltd, on double polished thick sections (about 100–150 μm thickness), at the University in Siena. Polishing media did not include diamond paste.

The laser spot size was focused to 1 μm with a 100× objective (Olympus BX40 miscroscope). The vertical resolution is estimated to be better than 10 μm. A polarized Ar^+-ion laser operating at 514 nm wavelength,

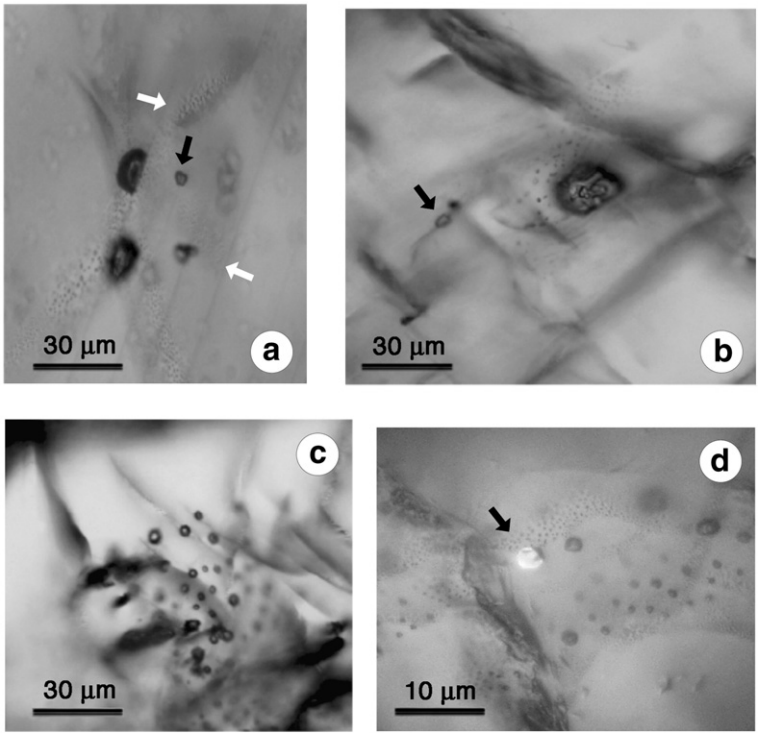

Fig. 1. Photomicrographs of fluid inclusions in clino-and ortho-pyroxene from Hawaiian xenoliths, representing early trapped fluids. a) Early fluid inclusions: small CO_2-rich superdense fluid inclusion (black arrow), and large decrepitated inclusions cut by spinel lamellae from the host clinopyroxene (white arrows). b) Large decrepited inclusion in clinopyroxene, and high-density/superdense CO_2-rich inclusion (black arrow). c) Group of small superdense CO_2-rich inclusions in orthopyroxene. d) Rounded mg-calcite inclusion (black arrow) within a trail of high-density and superdense CO_2-rich inclusions. Crossed polarizer.

and 400–600 mW incident power was used as the excitation source. The estimated spectral resolution is 1.5 cm^{-1} in the range between 100 and 4000 cm^{-1}. Acquisition times varied between 30 and 180 sec., and the number of acquisitions varied between 1 and 8. Daily calibration was performed by using the 1332 cm^{-1} diamond band. H_2S and CO_2 fluid relative concentrations (in mol%) were calculated from peak areas, considering both the different Raman polarizability of these gases, and the instrumental efficiency at the different wavelengths. Diamonds were detected in four out of eight rock samples.

3.1. Diamonds

The exceptional nature of early fluid trapped in inclusions has been confirmed by the present Raman study, since they often contain diamond, which has been detected by the typical sharp vibration at 1332 cm^{-1} (Fig. 2a, b). The diamond signal does not arise from outside the inclusions, as it disappears on moving the laser beam into the surrounding host mineral. Similarly, the diamond signal does not come from the upper surface of the section, because the confocal capability of the analytical system allows a vertical resolution within 10 µm from the focus depth.

The diamond spectrum is, however, surprisingly weak, considering the strong polarization of this phase. An additional peculiar feature is represented by both the broadening and the shift of the main vibration to lower frequency and down to 1329 cm^{-1}, whenever the vibration characteristic for highly-ordered high-temperature graphite – at about 1590 cm^{-1} – is observed (Fig. 2c, d). The Raman scattering cross section of diamond is 75 times smaller than that of graphite, which indicates that when the peaks due to diamond and graphite are of similar intensities, as in Fig. 2c and d, the concentration of the latter is only about 1%.

A possible interpretation for the above features is that diamonds are sub-micrometer in size (Yoshikawa et al., 1995; Gruen, 1999; Prinsloo, 2001), which might also explain why diamonds were never optically detected within fluid inclusions. Both the shifting of the 1332 cm^{-1} vibration to lower frequencies, and the incipient graphite formation could be related to size-dependent diamond-to-graphite transformation processes at high T, in the graphite

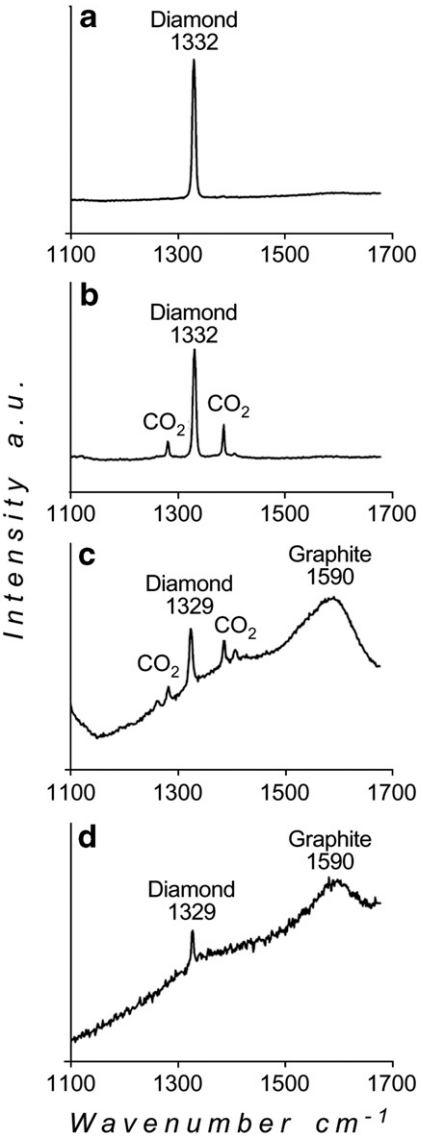

Fig. 2. Raman spectra of diamonds within fluid inclusions. a) Diamond main vibration at 1332 cm^{-1} in a decrepitated fluid inclusion. b) Diamond and CO_2 vibrations (at 1385 and 1280 cm^{-1}) in a high-density fluid inclusion. c) Diamond (1329 cm^{-1}) and graphite (1590 cm^{-1}) within high-density fluid inclusion. d) Diamond and graphite vibrations in a decrepitated fluid inclusion. a.u. = arbitrary units.

stability field, as observed during short (i.e. day-time scale) heating experiments at high pressure (Qian et al., 2001).

3.2. CO_2–H_2O–H_2S fluids

Preserved early fluid inclusions±diamonds contain high density to superdense CO_2-rich fluids (Figs. 3 and 4). Superdense CO_2 (d>1.178 g/cm^3) can be easily identified by its Raman spectroscopic features illustrated in Fig. 3a, including increased distance between the two main vibrations (Δ>106 cm^{-1}), shifting of peaks to lower wave numbers, increased peak intensity ratio, broadened peak bases, and flattened hot bands (van den Kerkhof and Olsen, 1990; Frezzotti et al., 1992). The distance between the two main Raman peaks (Δ) has been used to calculate CO_2 densities, using the equation proposed by (Kawakami et al., 2003). Obtained density values range from 0.94 to 1.21 g/cm^3 (Fig. 3), in agreement with previous microthermometry-based estimates (Frezzotti et al., 1992).

Raman analyses further show the presence of dissolved H_2O and H_2S, within the CO_2. The dominant features of the spectra are illustrated in Fig. 4: vibrational bands at 2608 cm^{-1} and 3638 cm^{-1} are present, which are characteristic of high-density H_2S, and of OH^- stretching vibrations for H_2O, respectively. The Raman spectrum of water contained within the CO_2 is typical for isolated molecules, as observed in low-density vapor (Dubessy et al., 1992): the symmetric shape for the OH^- band at 3638 cm^{-1} and its small width (15 cm^{-1}) suggest the absence of hydrogen bonds between molecules (i.e. water–water molecular interaction) (Fig. 4). Liquid water has not been detected.

Quantitative Raman analyses indicate additional 0.2 to 1 mol% H_2S within the CO_2 fluid. It is not possible to quantify the amount of water. However, since H_2O solubility in high-density CO_2 at room P–T condition is very low and estimated at 0.5 mol%, this value represents the minimum water content of CO_2-rich fluid inclusions.

3.3. Carbonates

The rare birefringent carbonates present within early CO_2±diamond inclusions consist of dolomite, while single carbonate inclusions range in composition from dolomite to Mg-calcite, this last one identified by its characteristic vibrations at 1089, 712, 281 and 156 cm^{-1} (Fig. 5). Carbonates within CO_2 fluid inclusions in mantle rocks, often represent a secondary assemblage formed via the interaction of the CO_2 fluids with the host mineral (i.e. magnesite in orthopyroxene, and dolomite in clinopyroxene step-daughter minerals). Raman analyses indicate that carbonates are primary features since dolomitic and Mg-calcitic compositions are observed in both orthopyroxene and clinopyroxene grains, excluding a genesis via CO_2 fluid-host mineral reactions.

Raman analyses further allow us to discriminate between the spectra of carbonates contained within fluid inclusions (Fig. 5a), and the spectra of single carbonates inclusions (Fig. 5b). When carbonates are present within

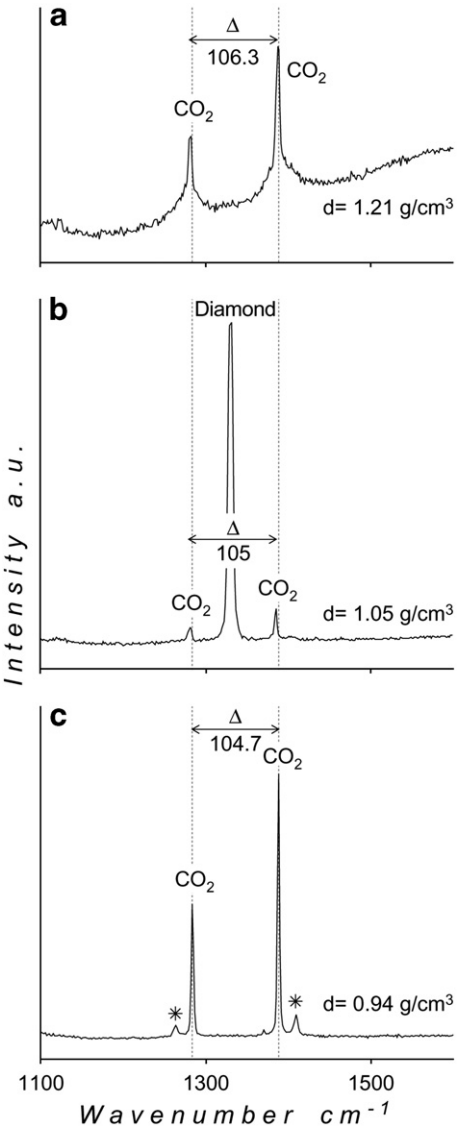

Fig. 3. Raman spectra of high density and superdense CO_2 fluid inclusions in the 1100–1300 cm^{-1} region. The distance between the two main Raman peaks (Δ) has been used to calculate CO_2 densities (Kawakami et al., 2003). a) Raman spectrum of superdense CO_2 (d>1.21 g/cm^3) inclusion in clinopyroxene (compare with 3c). The Raman spectrum shows distinctive features including increased distance between the two main vibrations (Δ=106.3 cm^{-1}), shifting of peaks to lower wave numbers, increased peak intensity ratio, broadened peak bases, and flattened hot bands. b) High density CO_2 (d=1.05 g/cm^3) inclusion containing diamond in clinopyroxene. c) Reference Raman spectrum for high density CO_2, showing two main vibrations (Fermi diad) at 1388 and 1285 cm^{-1}, split by Fermi resonance. Hot bands next to Fermi diad (asterisks) arise from excited vibrational states, due to the thermal energy of molecules. Δ = Frequency separation between the two main CO_2 vibrations, in cm^{-1}. d = density. a.u. = arbitrary units.

CO_2 fluid inclusions, the main carbonate vibration (1098 cm^{-1} for dolomite in Fig. 5a) results in wide halfwidths (full width of the Raman vibrations at half maximum height), which may be considered indicative of low crystallinity.

4. Discussion

4.1. Composition of the fluids contained within inclusions

The dominant fluid association preserved within early inclusions consist of high-density to superdense CO_2, with minor H_2S and H_2O. Several inclusions further contain nanocrystalline diamonds, and a few inclusions preserve the multiphase assemblage CO_2+dolomite+diamond. The presence of Mg-calcite and dolomite rounded inclusions indicate that carbonate-rich liquids might have been trapped within inclusions, and suggest for the existence of carbonate melts, that are unstable at the P–T conditions of most mantle xenoliths.

Nanocrystalline diamonds, although common, were not systematically detected in each high-density fluid inclusion, which implies that they cannot be considered daughter minerals (i.e. precipitated from the CO_2 or carbonate melt after trapping in the inclusions), while it rather suggests that diamonds where present as (xeno) crystals within the CO_2-rich fluid or melt. Incipient diamond-to-graphite transformation observed in some diamonds testifies only for re-equilibration during a short heating event, probably related to the ascent of pyroxenites in alkali-basaltic magmas.

Among the fluid phases preserved within inclusions, CO_2 is by far the dominant specie. The Raman detection of H_2O as molecules dissolved within the CO_2, however, might indicate that inclusions also contain (or have contained) some water (i.e. CO_2–H_2O inclusions). A liquid water film coating the cavity walls has never been observed, but in such small inclusions (3–5 μm in size) a water film of a thickness of 0.2 μm – corresponding to about 20 mol% of H_2O – cannot be identified by optical microscopy or by Raman spectroscopy. Thus, as much as 20 mol% of liquid water could be present as submicrometer-sized film wrapping the CO_2 fluid, and remain unnoticed. Alternatively, presence of water molecules dissolved within CO_2 might indicate that water was originally present in the high density fluid, but lost at later stage from fluid inclusions.

Fluid inclusions formed at high pressures and temperatures inevitably suffer various kind of secondary processes, resulting in a change of density and/or composition. There are many ways for a selective H_2O

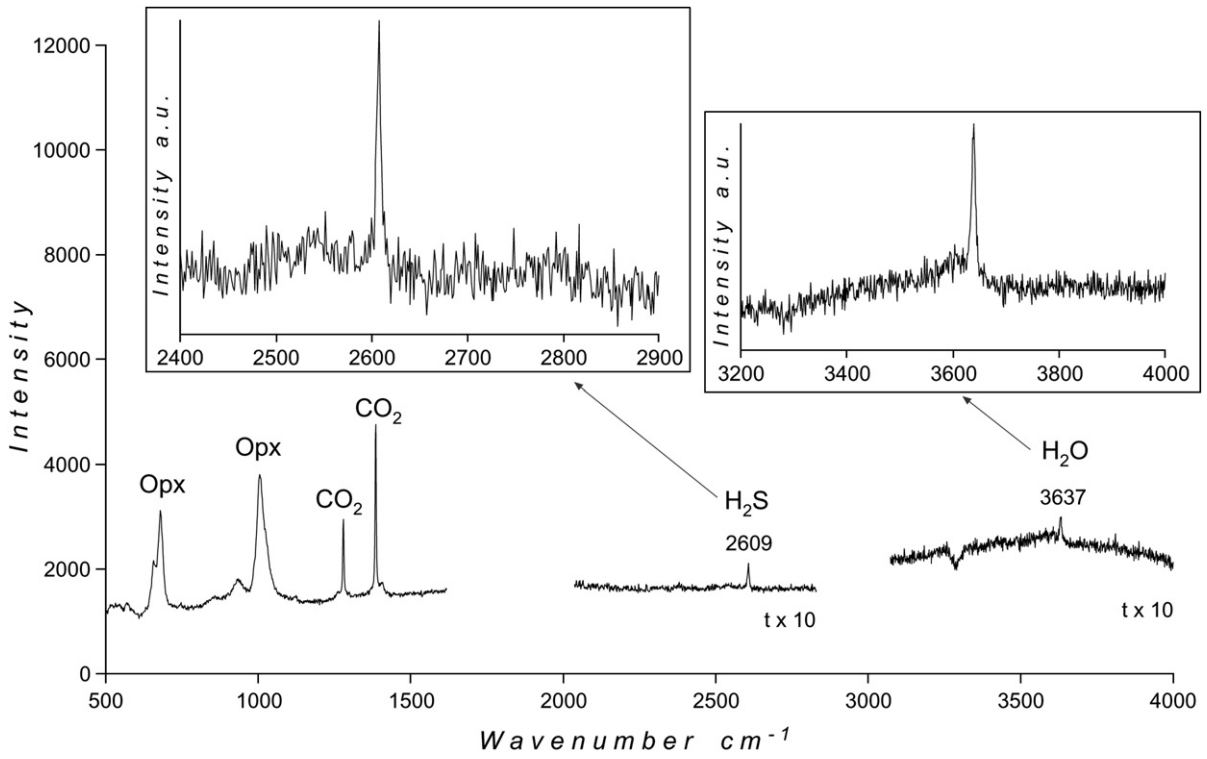

Fig. 4. Complete Raman spectrum in the 0–4000 cm^{-1} region for a high density CO_2–H_2O–H_2S fluid inclusion. The H_2O spectrum displays the typical vibrations for isolated water molecules within high density CO_2 fluids, see text. The Raman vibration for H_2S at 2609 cm^{-1} is indicative of high density. $t \times 10$ = ten time longer acquisition.

removal from fluid inclusions during the evolution of mantle minerals, including fluid-inclusion decrepitation, selective water-leakage through dislocations, H_2 diffusion, and chemical reactions with host minerals at low temperature, producing talc-like phases (Andersen and Neumann, 2001; Frezzotti et al., 2002b). The presence of common micro-cracks around single inclusions suggests that if water was present, it could have been lost by fluid inclusion decrepitation.

Thus, although we cannot quantify the various fluid components, our data provide compelling qualitative evidence for trapping of deep COHS high-density fluids or melts carrying diamond in the upper mantle beneath Oahu. This is an important point for our understanding of the mantle metasomatic processes, of the physical properties of the upper mantle beneath Hawaii, and ultimately of the conditions of genesis for magmatism at Hawaii.

4.2. Deep diamond-bearing COHS±carbonate inclusions: the carbonate-melt/CO_2 connection

In garnet pyroxenites, the crystal chemistry and the textural relation to orthopyroxene exsolutions indicate that early fluid inclusions formed prior to subsolidus cooling of xenoliths with exsolution of orthopyroxene and garnet, at pressures higher than about 3 GPa. This is greater than the estimated base of Cretaceous lithosphere at depths of about 85–90 km (Sen et al., 2005). Keshav and Sen (2001) reported majoritic garnet in pyroxenites from Salt Lake Crater which formed above the transition zones (6–8 GPa). Wirth and Rocholl (2003) identified nano-diamonds in silicate-melt inclusions within garnet pyroxenites. In addition, a deep (i.e. non-lithospheric) source for water, CO_2, and other fluid components beneath Hawaii was previously proposed by Sen et al. (1996, 2005), based on the restriction of hydrous and carbonate phases to deep xenoliths (i.e. garnet stability field) and their absence in shallower level rocks. Thus, the conclusion that some of the garnet pyroxenites formed at pressures higher than 4–5 GPa is validated by present identification of diamond within superdense CO_2 fluid inclusions.

At sub-lithospheric depths in the diamond stability field (>150 km), a COHS fluid phase could be either a CO_2-rich liquid (i.e. carbonate-melt) containing water and S, or a CH_4–H_2O–H_2S fluid, depending on local fO_2 conditions (Green and Falloon, 1998; Presnall and

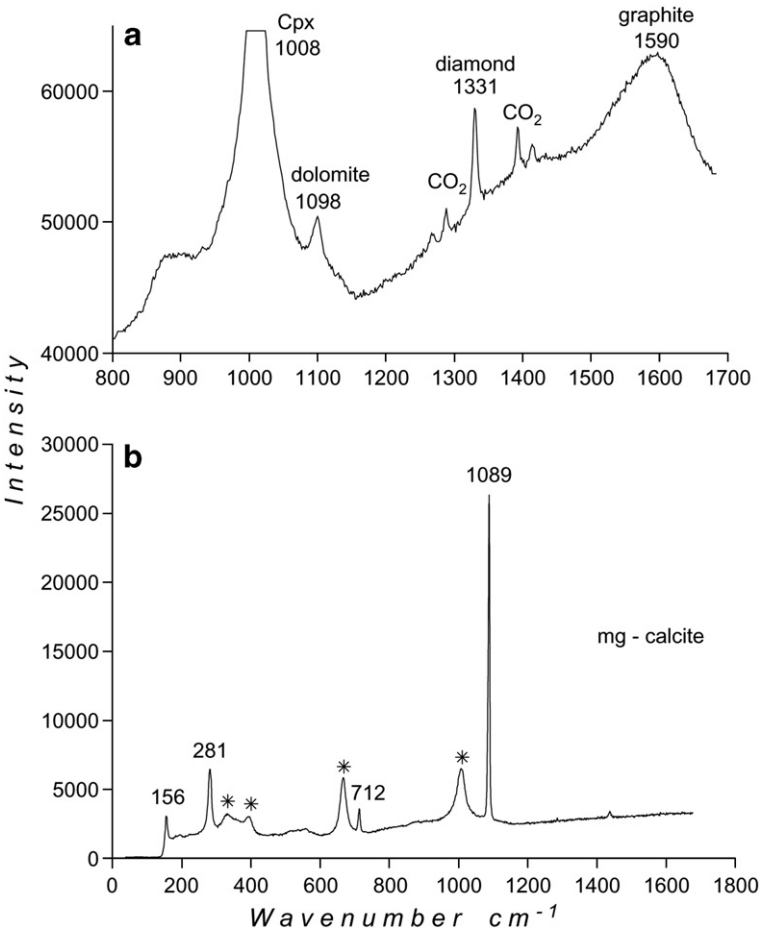

Fig. 5. Raman spectra of carbonates in inclusions. a) Raman spectrum in the region 800–1700 cm^{-1} of dolomite (1098 cm^{-1}) within a CO_2+diamond (1332 cm^{-1})+graphite (1590 cm^{-1}) inclusion (size 10 μm) in clinopyroxene. The wide halfwidths (full width of the Raman band at half maximum band height) of the main dolomite Raman vibration testifies for poor crystallinity. b) Raman spectrum in the region 0–1800 cm^{-1} of a rounded Mg-calcite inclusion (size 5 μm) in clinopyroxene. Asterisks indicate clinopyroxene contribution to the mg-calcite Raman spectrum.

Gudfinnsson, 2005; Dasgupta and Hirschmann, 2006). At these pressures, CO_2 is not stable and reacts with olivine to produce enstatite+magnesite (Newton and Sharp, 1975; Katsura and Ito, 1990). If enough CO_2 is supplied, the mantle equilibrium assemblage is olivine-free (garnet+pyroxenes). The investigated garnet pyroxenites do contain olivine, excluding a scenario of trapping of deep CO_2 fluids within fluid inclusions.

We propose that hydrous carbonate melts were present in the mantle beneath Hawaii at depths higher than 150 km. Rounded dolomite inclusions associated to CO_2 and diamond (Fig. 1d) are considered as direct remnants of a pristine fluid or melt phase present in the rocks at high pressures in the mantle. Similar COH fluids/melts do catalyze diamond growth (Pal'yanov et al., 1999; Akaishi et al., 2000), and the P–T conditions of spontaneous nucleation of octahedral diamonds are 5.6 GPa (160 km) at 1150 °C (Pal'yanov et al., 1999). The growth of diamonds proceeds either via precipitation of carbon from a CO_2-rich fluid/melt, or through CO_2-rich fluid/melt–peridotite interaction. Addition of water enhances the efficacy of diamond growth from such fluids (Pal'yanov et al., 1999).

Most mantle carbonate melts are ephemeral as either they will be consumed during reactions with the mantle wall rocks (Wallace and Green, 1988), and/or they undergo rapid decarbonation upon decompression (Canil, 1990). We interpret the superdense CO_2 inclusions, having formed as a result of decarbonation processes from an originally homogeneous high-volatile carbonate-rich melt. Superdense CO_2 inclusions might have originated either following decrepitation of carbonate-rich melt inclusions, or by trapping an outgassing carbonate melt. In either case, they contain a contribution

from of a carbonate component and give evidence for massive CO_2 degassing at depth.

In order to drive a carbonate-rich melt to decompose releasing CO_2 fluids ($\pm H_2O$), pressure conditions should have been <2 GPa, to allow decarbonation reactions (Wallace and Green, 1988; Yaxley and Green, 1996). The highest densities measured in CO_2 fluid inclusions containing diamonds fall in this pressure range (1.8 GPa). Since carbonates have been observed within superdense CO_2 inclusions, we propose that superdense and high-density CO_2 inclusions represent the fluid released during degassing of original carbonate inclusions during ascent of pyroxenites within the host magma at pressures below 2 GPa. At these pressures, CO_2 fluids have high wetting angles (Watson and Brenan, 1987), thus extremely low mobility. This might explain how part of the CO_2 originated via carbonate outgassing remained within inclusions in orthopyroxene and clinopyroxene grains. Thus, the poorly ordered carbonates detected within some of the high-density CO_2 inclusions may testify for incomplete outgassing processes (i.e. decomposing carbonates).

All together, CO_2 and carbonate inclusions provide evidence for a mode of deep mantle CO_2 inclusion formation, alternative to host basaltic magma degassing. It might be noteworthy to recall that any geobarometric data derived from similar inclusions might result robustly underestimated, since the density of CO_2 fluids merely reflects pressures of secondary processes (decarbonation), and not the original trapping of fluids as inclusions in mantle rocks at depth.

4.3. Origin of diamond-bearing carbonate-rich fluids/melts and comparison with other diamond-bearing melts beneath Hawaii

The data obtained as part of this study suggest that water-rich dolomitic melts were present at depths above 150 km in the mantle beneath Hawaii. No evidence for a silicate-melt component, either as inclusions or as glass microveins was observed in the studied rocks. However, silicate melt inclusions carrying nanocrystalline diamonds were previously identified in garnet pyroxenites from the same locality by (Wirth and Rocholl, 2003), based on transmission electron microscopy analyses.

The nature of the fluids/melts described by these authors is fully different: 1) diamonds are included in silicate glass containing variable amounts of carbonates (e.g. silicate melts enriched in CO_2). 2) Silicate melt inclusions show secondary (i.e. post-trapping) immiscibility processes forming a silicate–carbonate–CO_2 assemblage. 3) Melts have "basaltic" compositions, although silicate glasses show extremely variable chemistry, with silica ranging from 22 to 67 wt.%, and no apparent alkali enrichment (K_2O=0.1–0.6 wt.%; no Na_2O detected). 4) Silicate melt inclusions have high volatile contents, with Cl_2O from 0.5 to 2.9 wt.%, and SO_3 up 43 wt.%, suggesting the presence of a brine component. 5) Superdense CO_2 and/or carbonate inclusions are absent.

Therefore, at Salt Lake Crater, two distinct types of fluid/melt inclusions containing diamond record a compositional variability of the parental metasomatic fluids/melts. Since carbonate- and silicate-rich inclusions have never been found associated within the same rock sample, it is impossible to establish if these two melts are contemporaneous, and/or genetically related. The presence of diamonds, however, in both carbonate and silicate inclusions points to a common origin at depths greater than 150 km.

The apparent chemical discrepancy between the present data set and previously published data (Wirth and Rocholl, 2003) could be explained by petrogenetic models in the peridotite system, which predicate that carbonate and silicate fluids/melts parental to diamond growth can be genetically associated. In the upper mantle, carbonate-rich melts can result from different processes including: i) partial melting processes of a carbonated peridotite, ii) metasomatic reactions between a silicate–carbonate fluid/melt and mantle peridotite, and iii) local immiscibility processes in a carbonate-rich silicate melt (e.g. Schrauder and Navon, 1994; Schrauder et al., 1996; Lee and Wyllie, 1998; Navon et al., 2003). In the studied inclusions there is no evidence for a silicate component in the fluid/melt system: CO_2 and carbonate inclusions do not contain any silicate glass component, and have never been observed associated with silicate melt inclusions. Thus, we exclude the formation of carbonate-rich and silicate-rich end-members by local immiscibility processes.

Carbonate-rich melt can be generated at pressures above 1.9 GPa by very low degrees of partial melting (<1%) of a carbonated peridotite (Dalton and Presnall, 1998; Presnall and Gudfinnsson, 2005; Dasgupta and Hirschmann, 2007). At high-pressures in the diamond stability field, the carbonated-peridotite (±hydrous phases) solidus is dramatically depressed (ex. of about 600 °C at 6 GPa; Fig. 6), and low fractions of melts generated close to the solidus are dolomitic (i.e. Mg/Ca=1), and may contain variable amounts of H_2O and alkalies. Fig. 6 illustrates the progressive variation in melt composition with increasing temperature from dolomitic, through intermediate carbonate–silicate, to alkali-silicate (kimberlitic) in a 200 °C interval above

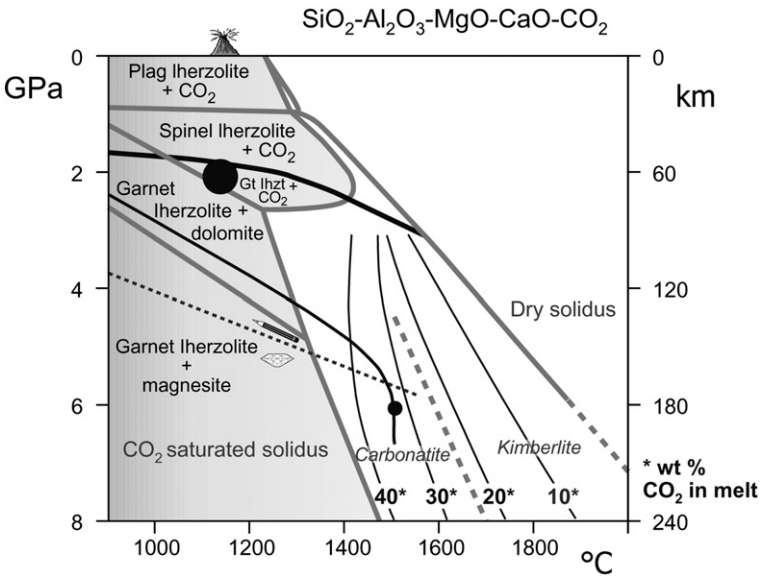

Fig. 6. Pressure–temperature diagram, showing the effects of CO_2-carbonate on mantle peridotite melting (SiO_2–Al_2O_3–MgO–CaO–CO_2) modified after (Dalton and Presnall, 1998; Presnall and Gudfinnsson, 2005), see text. The Effect of carbonates on the composition of melts generated at increasing temperature is indicated (white field). Subsolidus phase equilibria are illustrated in the gray field. Black line: Geotherm after (Sen et al., 2005). Large black circle: P–T conditions recorded by superdense CO_2 fluid inclusions generated by carbonate inclusion outgassing.

the solidus, as experimentally determined (Dalton and Presnall, 1998; Gudfinnsson and Presnall, 2005).

Alternatively, carbonate-rich melts might be generated by reaction between the mantle minerals and a volatile-rich carbonated silicate magma, during metasomatic processes at decreasing temperature (Schrauder and Navon, 1994). Progressive crystallization of silicate minerals from the metasomatic silicate melt may result in a carbonate-rich fluid with strong enrichment in alkali and incompatible elements.

Based on present data, it is not possible to discriminate whether carbonate and silicate melts represent melts generated by different degrees of melting of a carbonated peridotite at increasing temperature, or they derive one from the other through metasomatic reactions. However, since the preservation of diamonds indicate that no substantial heating events occurred during mantle evolution of fluids/melts at high pressures, we can speculate that carbonate-rich melts containing diamonds represent the products of (carbonate-rich) silicate melt/peridotite reactions on cooling. In this hypothesis, diamond would be generated during metasomatic reactions with mantle rocks.

4.4. Role of COHS fluids in mantle evolution beneath Hawaii

Present evidence for water-bearing carbonate melts, generated by metasomatic reactions or by mantle melting at pressures within the diamond stability fields, can be used to model the lithosphere–asthenosphere evolution beneath Hawaii. Post-erosional Hawaiian magmatism has been attributed to a resident anomalously fusible mantle recently metasomatized by low-degree (<2%) enriched partial melts (Yang et al., 2003). The data described here provide direct evidence for an asthenosphere locally saturated by COHS fluids or melts which are concentrated in pyroxenite rocks.

Carbonate-rich melts are highly mobile, and able to rise through the asthenosphere along a interconnected network, implanting at the base of the lithosphere and heterogeneously metasomatize the mantle, forming an enriched lithosphere (i.e. crystallization of carbonates ± hydrous minerals such as amphibole and phlogopite, and enrichment in LREE and incompatible trace elements), at pressures equal or close to the inferred source depths of HV, in which the studied xenoliths occur.

The effect of CO_2 on melting of peridotite is substantial, and differs from H_2O. When hydrous phases are present, dehydration melting reactions "control" the peridotite *solidus* temperature; conversely, if water is present dissolved in nominally anhydrous minerals, the solidus of peridotite is progressively decreased at increasing water content (Kawamoto and Holloway, 1997; Aubaud et al., 2004). Nominally volatile-free minerals do dissolve only a few ppm CO_2 (Keppler et al., 2003). Thus, carbonates are easily formed in the mantle at very low CO_2 concentrations, and, as shown in

Fig. 6, abruptly induce a sharp decrease in peridotite partial melting temperatures, at pressures >1.9 GPa.

The water concentration of Hawaiian mantle has been estimated to be about 400 to 600 ppm (Dixon et al., 1997; Wallace, 1998; Dixon and Clague, 2001), and the different OH^- solubility in mantle minerals indicates that the mantle in oceanic settings is saturated with 1000–4000 ppm, depending on pressure (Aubaud et al., 2004; Presnall and Gudfinnsson, 2005): thus, only if very heterogeneously distributed, 400–600 ppm of water are sufficient to locally saturate the mantle. The CO_2 concentration has been estimated to be about 1000 to 4000 ppm (Dixon et al., 1997), allowing the formation of carbonates.

Thus, the presence of a CO_2-dominated fluid in the Hawaiian mantle and its nearly worldwide presence, at least in the oceanic mantle, assures very low melting in the low-velocity zone, regardless of H_2O. As recently suggested (Presnall and Gudfinnsson, 2005; Dasgupta and Hirschmann, 2006), is actually CO_2, not H_2O, that represents by far the most important control on both the temperature of melting of peridotite, and on the composition of the melt produced.

5. Conclusions

High density to superdense CO_2–H_2O–H_2S inclusions containing diamond have been identified by Raman studies in garnet pyroxenites from Oahu, Hawaii. The characteristics of the fluids contained within inclusions are consistent with a genetic link with ephemeral carbonate-rich melt generated in the asthenosphere, at depth >150 km, within the diamond stability field.

Carbonate-rich fluids or melts are important metasomatic agents able for element and volatile transport to the lithospheric mantle: any model for mantle characterization at Hawaii must take into account the major effects that they have on lithosphere composition and physical properties. Fluids can have a great effect on shear-wave velocity (Bock, 1991), a factor which might explain the seismic tomography images of the Hawaiian upper mantle.

Present data do not intend to exclude other possible sources of recent mantle melting and enrichment processes. We emphasize that asthenospheric (COHS-diamond) fluids or melts have now been identified in mantle rocks beneath Hawaii, which satisfy geochemical constraints of post-shield Hawaiian volcanism, producing an enriched source with lower solidus temperature than average mantle. A high volatile content in Hawaiian magmas could suggest that such an influx of asthenospheric carbonate melts was not limited to the recent evolution of the Hawaiian mantle, but could also have taken place during the main stages of the shield volcanism.

Acknowledgements

Studied samples belong to the Dale Jackson Collection of the National Museum of Natural History (Smithsonian Institutions, Washington). The authors acknowledge careful review on a previous version of the manuscript by J. A. Dixon, G. R. Foulger, D. C. Presnall, and G. Sen. Present review by O. Navon and an anonymous reviewer, and editorial handling by R.W. Carlson are acknowledged. The Raman facility is provided by PNRA, the Italian agency for scientific research in Antarctica. Research was supported by MURST (2004), and Siena University (PAR 2004) to M.L.F.

References

Akaishi, M., Kumar, M.D.S., Kanda, H., Yamaoka, S., 2000. Formation process of diamond from supercritical H_2O–CO_2 fluid under high pressure and high temperature conditions. Diam. Rel. Mat. 9, 1945–1950.

Andersen, T., Neumann, E.R., 2001. Fluid inclusions in mantle xenoliths. Lithos 55, 301–320.

Aubaud, C., Hauri, E.H., Hirschmann, M.M., 2004. Hydrogen partition coefficients between nominally anhydrous minerals and basaltic melts. Geophys. Res. Lett. 31, L20611. doi:10.1029/2004GL021341.

Bock, G., 1991. Long-period S–P converted waves and the onset of partial melting beneath Oahu, Hawaii. Geophys. Res. Lett. 18, 869–872.

Canil, D., 1990. Experimental study bearing on the absence of carbonate in mantle-derived xenoliths. Geology 18, 1011–1013.

Dalton, J.A., Presnall, D.C., 1998. The continuum of primary carbonatitic–kimberlitic melt compositions in equilibrium with lherzolite: Data from the system CaO–MgO–Al_2O_3–SiO_2–CO_2 at 6 GPa. J. Petrol. 39, 1953–1964.

Dasgupta, R., Hirschmann, M.M., 2006. Melting in the Earth's deep upper mantle caused by carbon dioxide. Nature 440, 659–662.

Dasgupta, R., Hirschmann, M.M., 2007. Effect of variable carbonate concentration on the solidus of mantle peridotite. Am. Mineral. 92, 370–379.

Dixon, J.A., Clague, D.A., 2001. Volatiles in basaltic glasses from Loihi Seamount, Hawaii: evidence for a relatively dry plume component. J. Petrol. 42, 627–654.

Dixon, J.E., Clague, D.A., Wallace, P., Poreda, R., 1997. Volatiles in alkalic basalts from the North Arch Volcanic Field, Hawaii: extensive degassing of deep submarine erupted alkalic series lavas. J. Petrol. 38, 911–939.

Dubessy, J., Boiron, M.C., Moissette, A., Monnin, C., Sretenskaya, N., 1992. Determination of water, hydrates and Ph in fluid inclusions by micro-Raman spectrometry. Eur. J. Mineral. 4, 885–894.

Frezzotti, M.L., Burke, E.A.J., De Vivo, B., Stefanini, B., Villa, I.M., 1992. Mantle fluids in pyroxenite nodules from Salt Lake Crater (Oahu, Hawaii). Eur. J. Mineral. 4, 1137–1153.

Frezzotti, M.L., Touret, J.L.R., Neumann, E.R., 2002a. Ephemeral carbonate melts in the upper mantle: carbonate–silicate immiscibility

in microveins and inclusions within spinel peridotite xenoliths, La Gomera, Canary Islands. Eur. J. Mineral. 14, 891–904.

Frezzotti, M.L., Andersen, T., Neumann, E.-R., Simonsen, S.L., 2002b. Carbonatite melt-CO_2 fluid inclusions in mantle xenoliths from Tenerife, Canary Islands: a story of trapping, immiscibility and fluid–rock interaction in the upper mantle. Lithos 64, 77–96.

Green, D.H., Falloon, T.J., 1998. Pyrolite: a Ringwood concept and its current expression. In: Jackson, J. (Ed.), The Earth's Mantle. Cambridge University Press, New York, pp. 311–378.

Gruen, D.M., 1999. Nanocrystalline diamond films. Annu. Rev. Mater. Sci. 29, 211–259.

Gudfinnsson, G.H., Presnall, D.C., 2005. Continuous gradations among primary carbonatitic, kimberlitic, melilititic, basaltic, picritic, and komatiitic melts in equilibrium with garnet lherzolite at 3–8 GPa. J. Petrol. 46, 1645–1659.

Izraeli, E.S., Jeffrey, W.H., Navon, O., 2004. Fluid and mineral inclusions in cloudy diamonds from Koffiefontein, South Africa. Geochim. Cosmochim. Acta 68, 2561–2575.

Kamenetsky, M.B., Sobolev, A.V., Kamenetsky, V.S., Maas, R., Danyushevsky, L.V., Thomas, R., Pokhilenko, N.P., Sobolev, N.V., 2004. Kimberlite melts rich in alkali chlorides and carbonates: a potent metasomatic agent in the mantle. Geology 32, 845–848.

Katsura, T., Ito, E., 1990. Melting and subsolidus phase-relations in the $MgSiO_3$–$MgCO_3$ system at high-pressure implications to evolution of the earth atmosphere. Earth Planet. Sci. Lett. 99, 110–117.

Kawakami, Y., Yamamoto, J., Kagi, H., 2003. Micro-Raman densimeter for CO_2 inclusions of mantle-derived minerals. Appl. Spectrosc. 57, 1333–1339.

Kawamoto, T., Holloway, J.R., 1997. Melting temperature and partial melt chemistry of H_2O-saturated mantle peridotite to 11 Gigapascals. Science 276, 240–243.

Keppler, H., Wiedenbeck, M., Shcheka, S.S., 2003. Carbon solubility in olivine and the mode of carbon storage in the Earth's mantle. Nature 424, 414–416.

Keshav, S., Sen, G., 2001. Majoritic garnets in Hawaiian xenoliths: preliminary results. Geophys. Res. Lett. 28, 3509–3512.

Keshav, S., Sen, G., Presnall, D., in press. Garnet-bearing xenoliths from Salt Lake Crater, Oahu, Hawaii; high-pressure fractional crystallization in the oceanic mantle. J. Petrology.

Klein-Ben David, O., Wirth, R., Navon, O., 2006. TEM imaging and analysis of micro-inclusions in diamonds — a close look at diamond-growing fluids. Amer. Min. 91, 366–375.

Lee, W., Wyllie, P.J., 1998. Petrogenesis of carbonatite magmas from mantle to crust, constrained by the system CaO–(MgO+FeO*)–(Na_2O+K_2O)–(SiO_2+Al_2O_3+TiO_2)–CO_2. J. Petrol. 39, 495–577.

Navon, O., Hutcheon, I.D., Rossman, G.R., Wasserburg, G.J., 1988. Mantle derived fluids in diamond micro-inclusions. Nature 335, 784–789.

Navon, O., Izraeli, E.S., Klein-BenDavid, O., 2003. Fluid inclusions in diamonds: the carbonatitic connection. 8th International Kimberlite Conference, 22–27 June 2003, Victoria, Canada, ext. abs., FLA-0107.

Newton, R.C., Sharp, W.E., 1975. Stability of forsterite+CO_2 and its bearing of the role of CO_2 in the mantle. Earth Planet. Sci. Lett. 26, 239–244.

Pal'yanov, Y.N., Sokol, A.G., Borzdov, Y.M., Khokhryakov, A.F., Sobolev, N.V., 1999. Diamond formation from mantle carbonate fluids. Nature 400, 417–418.

Presnall, D.C., Gudfinnsson, G.H., 2005. Carbonate-rich melts in the seismic low-velocity zone and deep mantle. In: Foulger, G.R., Natland, J.H., Presnall, D.C., Anderson, D.L. (Eds.), Plates, Plumes, and Paradigms. Geol. Soc. Am. Spec. Paper, 388, pp. 207–216.

Prinsloo, L.C., 2001. Radiation effects of ion beams in diamond: C Infrared and Raman spectroscopy. Appl. Phys., A Mater. Sci. Process. 72, 639–670.

Qian, J., Pantea, C., Voronin, G., Zerda, T.W., 2001. Partial graphitization of diamond crystals under high-pressure and high-temperature conditions. J. Appl. Phys. 90, 1632–1637.

Roedder, E., 1965. Liquid CO_2 inclusions in olivine-bearing nodules and phenocrysts from basalts. Am. Mineral. 50, 1746–1782.

Roedder, E., 1984. Fluid Inclusions. Mineral. Soc. Am., Rev. Mineral 12. 646 pp.

Schiano, P., Clocchiatti, R., Shimizu, N., Maury, R.C., Jochum, K.P., Hoffman, A.W., 1995. Hydrous silica-rich melts in the sub-arc mantle and their relationship with erupted arc lavas. Nature 377, 595–600.

Schrauder, M., Navon, O., 1994. Hydrous and carbonatitic mantle fluids in fibrous diamonds from Jwaneng, Botswana. Geochim. Cosmochim. Acta 58, 761–771.

Schrauder, M., Koeberl, C., Navon, O., 1996. Trace element analyses of fluid bearing diamonds from Jwaneng, Botswana. Geochim. Cosmochim. Acta 60, 4711–4724.

Sen, G., 1988. Petrogenesis of spinel lherzolite and pyroxenite suite xenoliths from the Koolau shield, Oahu, Hawaii: Implications for petrology of the post-eruptive lithosphere beneath Oahu. Contrib. Mineral. Petrol. 100, 61–91.

Sen, G., Macfarlan, A., Srimal, N., 1996. Significance of rare hydrous alkaline melts in Hawaiian xenoliths. Contrib. Mineral. Petrol. 122, 415–427.

Sen, G., Keshav, S., Bizimis, M., 2005. Hawaiian mantle xenoliths and magmas: composition and thermal character of the lithosphere. Amer. Min. 90, 871–887.

Thompson, A.B., 1992. Water in the Earth's Upper Mantle. Nature 358, 295–302.

van den Kerkhof, A.M., Olsen, S.N., 1990. A natural example of superdense CO_2 inclusions: microthermometry and Raman analysis. Geochim. Cosmochim. Acta 54, 895–901.

Wallace, P.J., 1998. Water and partial melting in mantle plumes: inferences from the dissolved H_2O concentrations of Hawaiian basaltic magmas. Geophys. Res. Lett. 25, 3639–3642.

Wallace, M.E., Green, D.H., 1988. An experimental-determination of primary carbonatite magma composition. Nature 335, 343–346.

Watson, E.B., Brenan, J.M., 1987. Fluids in the lithosphere, 1. experimentally-determined wetting characteristics of CO_2–H_2O fluids and their implications for fluid transport, host–rock physical properties, and fluid inclusion formation. Earth Planet. Sci. Lett. 85, 497–515.

Wirth, R., Rocholl, A., 2003. Nanocrystalline diamond from the Earth's mantle underneath Hawaii. Earth Planet. Sci. Lett. 211, 357–369.

Wyllie, P.J., Ryabchikov, I.D., 2000. Volatile components, magmas, and critical fluids in upwelling mantle. J. Petrol. 41, 1195–1206.

Yang, H.Y., Frey, F.A., Clague, D.A., 2003. Constraints on the source components of lavas forming the Hawaiian North arch and Honolulu volcanics. J. Petrol. 44, 603–627.

Yaxley, G.M., Green, D.H., 1996. Experimental reconstruction of sodic dolomitic carbonatite melts from metasomatised lithosphere. Contrib. Mineral. Petrol. 124, 359–369.

Yoshikawa, M., Mori, Y., Obata, H., Maegawa, M., Katagiri, G., Ishida, H., Ishitani, A., 1995. Raman scattering from nanometer-sized diamond. Appl. Physics Lett. 67, 694–696.